Ising Model for Phase Separation in Alloys with Anisotropic Elastic Interaction. I. Theory

Peter Fratzl[1] and Oliver Penrose
Department of Mathematics, Heriot-Watt University
Edinburgh EH14 4AS, U.K.

[1] permanent address:
Institut für Festkörperphysik der Universität Wien
A-1090 Wien, Boltzmanngasse 5, Austria

Abstract

We propose a model to study, on an atomistic scale, the effects of elastic misfit strains on the growth and coarsening of domains in phase-separating alloys. The model considered is a two-dimensional square crystal lattice with periodic boundary conditions and with an A or B atom near each site. To model the elastic interaction, nearest and next-nearest neighbors are connected by springs with longitudinal and transverse stiffnesses. In addition, there is a chemical interaction between nearest neighbours, favouring like against unlike pairs. A mean field analysis predicts phase separation into coherent phases, below a temperature which (for a typical set of elastic parameters) increases with the strength of the elastic forces. This critical temperature is less than that for separation into incoherent phases. The analysis also predicts how the anisotropy determines the shapes of domains at early times. A Monte Carlo procedure for implementing Kawasaki dynamics to represent diffusion in this model is described.

1 Introduction

The effect of elastic misfit strains on the growth and coarsening of domains in phase-separating alloys has been studied intensively in recent years, both theoretically [1-14] and experimentally [2,15-24] There are two main types of effect: on the shapes of the domains, and on the rate at which they grow in size. On the one hand the domains can, for example, be cuboidal or plate-like at alloy concentrations where they would otherwise be spherical; on the other, the rate of growth of the domains can be considerably slowed down, particularly in the later stages where it may almost come to a complete stop. The latter effect could be important for practical applications since an alloy whose microstructure coarsens too rapidly during service at high temperatures will eventually become mechanically weak. Generally the two effects may occur together, so that it is difficult to sort out their causes, whether theoretically or experimentally. However, it is possible to observe the two effects separately. Thus, in some nickel-based superalloys the shapes and the arrangement of the domains are strongly affected by the misfit in lattice spacing between matrix and precipitates, yet the rate of growth appears to be unaffected by elastic interactions [22, 20, 25]. On the other hand in Ti-Mo alloys, the domains are nearly spherical, but the coarsening stops after the precipitates reach a certain size [23, 24].

It is known [1] that if the elastic interactions are isotropic and independent of concentration, then in an infinite sample with linear elasticity there is no elastic interaction between misfitting domains. This result suggests two possible explanations for the observed elastic effects : one is that the elastic interactions may depend on direction (anisotropy), the other that they may depend on composition. Although there is no real proof, it appears that the anisotropy is the cause of the non-spherical shape of the domains and their ordered arrangement and that the composition dependence is mostly the cause of the slowing-down of domain coarsening.

There are various ways to study this problem theoretically. One way [1, 13, 11] is to treat the domains as macroscopic objects of some simple shape, usually a sphere, with a sharp interface. The ingredients of the theory are the interface energy, the elastic interactions (calculated by solving the equations of macroscopic elasticity) and mass transport from one domain to another (calculated by solving a diffusion equation). A second method [4-8] is more microscopic, using a mean-field description. The local state of the material is described by two fields: the concentration and the elastic displacement. The free energy is written as a functional of these two fields and is minimized with respect to the elastic displacements. The resulting "reduced" free energy is a functional of the concentration field only, with a long-range interaction. The interdiffusion is then treated exactly as in the original Cahn-Hilliard theory of spinodal decomposition [4, 26].

A different microscopic approach was used by Gayda and Srolovitz [14]. They did Monte Carlo simulations in which domains were represented by sites of an Ising model, with an isotropic composition-dependent elastic interaction whose magnitude was calculated by numerically solving the equations of continuum elasticity. The interdiffusion was modelled by allowing neighbouring domains to change places — Kawasaki spin-exchange dynamics, in Ising model terminology.

The purpose of the present paper and its sequel is to simulate the effect of elastic interactions using a fully microscopic model in which atoms are individually represented.

The model we shall use is an Ising model. In the absence of elastic interactions, the Ising model has been found to give excellent account of both the microstructural evolution and the growth kinetics of alloys undergoing phase separation [27]; for instance, the self-similarity law for the evolution of the alloy microstructure was first discovered for the Ising model [28] and only later confirmed for many real alloys. At the same time, there is a well-developed microscopic theory for the elasticity of crystal lattices [29-31]. In the present paper we combine these two models by treating the crystal as a mixture of two types of atom, with two distinct kinds of interaction, a "chemical" interaction depending only on the identities of the two interacting atoms and an "elastic" energy depending on their displacements away from their lattice positions as well. We consider only the two-dimensional square lattice and derive a Hamiltonian that is simple enough to permit efficient computer simulations, yet still contains the essential features of the elastic interaction potential. In the present paper we also investigate the phase diagram and the dynamical properties of this model using a mean field approximation. In the following paper we use Monte Carlo computer experiments to investigate the evolution of the microstructure after a quench into the miscibility gap.

2 Description of the model

Our model for a crystalline solid is a lattice (with periodic boundary conditions) where each of the N sites is occupied by either an A or a B atom. We define a "spin" function $\gamma(\mathbf{p})$ by $\gamma(\mathbf{p}) = 1$ if there is an A-atom at site $\mathbf{p}$ and $\gamma(\mathbf{p}) = -1$ if there is a B-atom at this site. The atoms are assumed to interact "chemically" over short distances, with like atoms attracting one another. When combined with an appropriate dynamical assumption, for example Kawasaki dynamics [32], this assumption gives a model for the phase separation process in alloys where A and B atoms are of the same size. If the atoms are of different sizes, however, elastic interactions will be important. To model these, we shall use the model first studied by Born and Huang [29], in which atoms make small vibrations about their equilbrium positions and where the interatomic forces are modeled by assuming that pairs of atoms are joined by linear springs. For any given arrangement of A and B atoms over the N lattice sites, it is assumed that the atoms take up the positions near their assigned lattice sites that minimize the elastic energy, so that the energy can be expressed in terms of the arrangement of atoms, that is on the function $\gamma(\mathbf{p})$. Khachaturyan [30] and Cook and deFontaine [31] have shown how the minimized elastic energy for the mixture can be written in the form

$$E^{el} = \frac{1}{2N} \sum_{\mathbf{k} \neq 0} E(\mathbf{k})\, |\Gamma(\mathbf{k})|^2 + \text{const.} \tag{1}$$

where the sum extends over the first Brillouin zone of the lattice and where we define

$$\Gamma(\mathbf{k}) = \sum_{\mathbf{p}} \gamma(\mathbf{p}) e^{i\,\mathbf{p}\cdot\mathbf{k}} \tag{2}$$

The "elastic potential" $E(\mathbf{k})$ can be calculated for any type of lattice, and has been given explicitly for some, e.g. in [31].

If the domains are very large compared to the lattice spacing, the $\mathbf{k}$-values contributing to the sum in (1) are all very small; then $E(\mathbf{k})$ can be replaced by its limiting form for small $|\mathbf{k}|$, which depends only on the direction of the vector $\mathbf{k}$. In the theory of Khachachuryan [30] this limiting form depends only on the elastic constants of the material. Its has been shown [8] that many features of alloy decomposition can be studied this way. If, however, one is to study the formation of rather small precipitates as, e.g., Guinier-Preston zones [15], the crystalline character of the solid cannot be neglected and the dispersion of E, i.e. its dependence on $|\mathbf{k}|$, has to be taken into account.

2.1 Calculation of the elastic potential

For the simulations to be described here we consider a two-dimensional crystal with one atom near each site of a finite square lattice. To model the elastic interactions, we suppose all the nearest-neighbour pairs of atoms to be connected by springs, with longitudinal stiffness L_+ and transverse stiffness T_+. In addition, the next-nearest neighbour pairs are connected by springs with longitudinal stiffness $L_\times$ and transverse stiffness zero (see Fig 1). As we shall see, (eqn (3) below) these three stiffness constants give just enough freedom to fit the three independent elastic constants of a general crystal having the symmetry of the square lattice. Further springs connecting more distant pairs of neighbours could be introduced, but we think they would not lead to anything essentially new. The non-zero transverse stiffness T_+ has to be included because of Cauchy's relation [29] which holds for the elastic constants for a crystal with purely central forces but not for those of real metallic crystals.

A possible objection to this model is that the law governing the transverse forces exerted by the springs is not rotationally invariant. It is shown in Appendix 1, however, that so long as the lattice spacing a remains fixed the energy of the entire crystal given by this model is the same as for a different model in which the interactions do obey rotationally invariant laws. In the limit where the particle displacements vary only slightly form one lattice site to the next, the latter model becomes equivalent to a elastic continuum, whose elastic constants are related in the following way to the spring stiffnesses in the model we actually use:

$$\left\{ \begin{array}{ll} c_{11} & = L_\times + L_+ \\ c_{44} & = L_\times + T_+ \\ c_{12} & = L_\times - T_+ \end{array} \right. \tag{3}$$

A useful combination of these elastic constants is the bulk modulus, which in two dimensions is

$$B = \frac{1}{2}(c_{11} + c_{12}) = L_\times + \frac{1}{2}(L_+ - T_+) \tag{4}$$

For our numerical work we had to choose particular values for the stiffness constants $L_+, T_+, L_\times$. We chose these so as to make the corresponding elastic constants c_{11} etc. proportional to those for copper; these numerical values are given in Table 1. Although one of the stiffness constants chosen is negative, there is no instability since the total energy (eqn (6) below) is still positive definite.

To account for the difference in size of the A and B atoms, we suppose that the atoms are spheres (or circles) and that the ends of the springs are attached at the surfaces of these spheres. The radius of the sphere at site $\mathbf{p}$ is thus

$$R(\mathbf{p}) = \frac{1}{2}(R_A + R_B) + \frac{1}{2}(R_A - R_B)\,\gamma(\mathbf{p}) \tag{5}$$

where R_A and R_B are the radii of the A and B atoms. The position of the atom near the lattice site at $\mathbf{p}$ will be denoted by $\mathbf{p}+\mathbf{u}(\mathbf{p})$. Calculating the contribution of all the springs to the elastic energy and neglecting terms of order $|\mathbf{u}|^3$, we obtain, as shown in Appendix 2, for the total elastic energy

$$\begin{aligned} W &= \frac{1}{2}L_+ \sum_{\mathbf{p}} \sum_{i=1,2} \{(u_i(\mathbf{p}+a\mathbf{e}_i) - u_i(\mathbf{p}) - \eta_+(\mathbf{p}+a\mathbf{e}_i) - \eta_+(\mathbf{p})\}^2 \\ &+ \frac{1}{2}T_+ \sum_{\mathbf{p}} \{[(u_2(\mathbf{p}+a\mathbf{e}_1) - u_2(\mathbf{p})]^2 + [(u_1(\mathbf{p}+a\mathbf{e}_2) - u_1(\mathbf{p})]^2\} \end{aligned} \tag{6}$$

$$+\frac{1}{2}L_\times \sum_{\mathbf{p}} \sum_{\mu\in\{+1,-1\}} \left[\frac{u_1(\mathbf{p}+a\mathbf{e}^{(\mu)}) + \mu u_2(\mathbf{p}+a\mathbf{e}^{(\mu)}) - u_1(\mathbf{p}) - \mu u_2(\mathbf{p})}{\sqrt{2}} - \eta_\times(\mathbf{p}+a\mathbf{e}^{(\mu)}) - \eta_\times(\mathbf{p})\right]^2$$

where a is the lattice spacing, $\mathbf{e}_i$ denotes a unit vector in the i direction ($i = 1$ representing the row direction on the lattice and $i = 2$ the column direction), $\mathbf{e}^{(\mu)}$ means $\mathbf{e}_1 + \mu\mathbf{e}_2$, $u_1(\mathbf{p}), u_2(\mathbf{p})$ are the components of the vector $\mathbf{u}(\mathbf{p})$ in the 1 and 2 directions and $\eta_+, \eta_\times$ are given, in accordance with (A8) , by

$$\eta_+(\mathbf{p}) = R(\mathbf{p}) + \frac{l_+}{2} - \frac{a}{2}, \qquad \eta_\times(\mathbf{p}) = R(\mathbf{p}) + \frac{l_\times}{2} - \frac{a\sqrt{2}}{2} \tag{7}$$

It is fundamental to our method that we assume the atoms to come to thermal equilibrium with respect to their vibrational motion much faster than they can diffuse to new positions. At temperatures high enough for a classical treatment of the vibrations to be adequate, the thermodynamic equilibrium energy will be the sum of two parts: the minimum of W with respect to variations of the atomic displacements $\mathbf{u}(\mathbf{p})$ and the lattice spacing a, and a term $2NkT$ from the (two-dimensional) equipartion of energy. Since the latter does not depend on the arrangement of the A and B atoms over the lattice sites, we shall ignore it. To minimize W, we first consider variations of a with the $\mathbf{u}(\mathbf{p})$'s held fixed. This leads to an expression for a depending linearly on the overall concentration c of A atoms. When this expression is substituted into (7) we obtain

$$\eta_+(\mathbf{p}) = \eta(\mathbf{p}) + \eta_+^{(0)}, \quad \eta_\times(\mathbf{p}) = \eta(\mathbf{p}) + \eta_\times^{(0)} \tag{8}$$

where $\eta_+^{(0)}$ and $\eta_\times^{(0)}$ are independent of $\mathbf{p}$ but depend linearly on c. Explicit formulas for a, $\eta_+^{(0)}$ and $\eta_\times^{(0)}$ are given in Appendix 3. $\eta(\mathbf{p})$ is defined by

$$\eta(\mathbf{p}) = \frac{1}{2}(R_A - R_B)[\gamma(\mathbf{p}) - (2c-1)]. \tag{9}$$

This last definition is chosen so as to make the average of η over the whole lattice equal to zero.

Once the formulas (8) have been substituted into the formula (6) for the elastic energy, the resulting expression is to be be minimized with respect to the $\mathbf{u}(\mathbf{p})$'s. As shown in [31] the calculation is best done by first writing the right side of (6) in terms of the Fourier transforms of $\mathbf{u}(\mathbf{p})$ and $\eta(\mathbf{p})$ (the latter being proportional, for $\mathbf{k} \neq \mathbf{0}$, to the Fourier transform of $\gamma(\mathbf{p})$). Minimization with respect to the x and y components of the transform of $\mathbf{u}(\mathbf{p})$ then leads to a result similar to (1), namely

$$W_{min} = W_0 + \frac{1}{2N}(R_A - R_B)^2 \sum_{\mathbf{k}\neq 0} \Phi(\mathbf{k})\ |\Gamma(\mathbf{k})|^2 \tag{10}$$

where

$$W_0 = 4N(L_+ \eta_+^{(0)2} + L_\times \eta_\times^{(0)2}), \tag{11}$$

$\Gamma(\mathbf{k})$ is defined as in (2), and $\Phi(\mathbf{k})$ is defined by

$$\Phi(\mathbf{k}) = \Omega(\mathbf{k}) - \frac{N(\mathbf{k})}{2D(\mathbf{k})} \tag{12}$$

with

$$\begin{aligned} \Omega(\mathbf{k}) &= 2L_+ + 2L_\times - \frac{1}{2}(L_+ + 2L_\times)(v+w) + L_\times vw \\ N(\mathbf{k}) &= (L_+ v + T_+ w + L_\times(v + w - vw))\ (L_+ + \sqrt{2}\, L_\times(1-v))^2\ (2-w)w \\ &+ (L_+ w + T_+ v + L_\times(v + w - vw))\,(L_+ + \sqrt{2}\, L_\times(1-w))^2\ (2-v)v \\ &- 2L_\times\ (L_+ + \sqrt{2}\, L_\times(1-v))\ (L_+ + \sqrt{2}\, L_\times(1-w))\ (2-v)(2-w)vw \\ D(\mathbf{k}) &= (L_+ + L_\times)(L_\times + T_+)\ (v+w)^2 - L_\times(L_+ + T_+)\ vw(v+w) \\ &+ (L_+ + 2L_\times - T_+)(L_+ - 2L_\times - T_+)\ vw \end{aligned} \tag{13}$$

and

$$v = 1 - \cos(a\,k_1) \qquad \text{and} \qquad w = 1 - \cos(a\,k_2)$$

k_1 and k_2 being the components of the vector $\mathbf{k}$ along the rows and columns of the square lattice.

2.2 Long-wave limit

Most studies of phase separation kinetics under the influence of elastic misfit strain [4, 5, 8] have assumed that $\gamma(\mathbf{p})$ can be regarded as a slowly varying function of a continuous variable, so that $\Gamma(\mathbf{k})$ is concentrated near the origin in $\mathbf{k}$-space. In this case only the small-$\mathbf{k}$ limiting form of $\Phi(\mathbf{k})$ is needed. In terms of polar coordinates (k, θ) defined so that $k_1 = k\cos\theta, k_2 = k\sin\theta$ this limiting form is given by

$$Y(\theta) = \lim_{k\to 0} \Phi(\mathbf{k}) = 2L_+ + 2L_\times + \frac{(L_+ + \sqrt{2}\, L_\times)^2}{L_+ + L_\times}\, \hat{Y}(\theta) \tag{14}$$

where

$$\hat{Y}(\theta) = -\ \frac{4 + 2\,\Delta\ \sin^2(2\,\theta)}{4 + (1 + c_{12}/c_{11})\Delta\ \sin^2(2\,\theta)} \tag{15}$$

with c_{11}, c_{12} as in eqn (3) and Δ the anisotropy parameter defined by

$$\Delta = \frac{(c_{11} - c_{12} - 2c_{44})}{c_{44}} = \frac{L_+ - T_+ - 2L_\times}{T_+ + L_\times} \tag{16}$$

If the anisotropy parameter Δ is positive, then $Y(\theta)$ is a minimum when $\sin(2\theta)$ is as large as possible, i.e. when $\theta = \pm\pi/4$, indicating that the precipitate domains will tend to lie along the (11) or $(\bar{1}1)$ direction. For negative values of Δ the minimizing value of θ is 0 (or $\pi/2$), and the precipitates may be expected to prefer the (10) or (01) direction.

Equation (14) is similar to the corresponding expressions derived from elastic continuum models by Cahn [5] and Khachaturyan [3]. The expressions do not agree in detail because we make different assumptions about the way the sizes of the atoms affect the energy of the system.

2.3 Total Hamiltonian

The total Hamiltonian of our model system is the sum of the elastic interaction just described (eqn (10)) and a nearest neighbour attraction of magnitude J between like atoms:

$$E = W_0 + \frac{1}{2N}(R_A - R_B)^2 \sum_{\mathbf{k}} \Phi(\mathbf{k})\ |\Gamma(\mathbf{k})|^2 - \sum_{\mathbf{p},\mathbf{p}':|\mathbf{p}-\mathbf{p}'|=a} J\,\gamma(\mathbf{p})\gamma(\mathbf{p}') \tag{17}$$

with the convention

$$\Phi(\mathbf{0}) = 0. \tag{18}$$

This can be written as a double sum over lattice sites

$$E = W_0 + \frac{1}{2}\sum_{\mathbf{p}}\sum_{\mathbf{p}'} \psi(\mathbf{p} - \mathbf{p}')\,\gamma(\mathbf{p})\,\gamma(\mathbf{p}') \tag{19}$$

where

$$\psi(\mathbf{p}) = \begin{cases} (R_A - R_B)^2\phi(\mathbf{p}) - J & \text{if } \mathbf{p} \text{ connects nearest neighbours} \\ (R_A - R_B)^2\phi(\mathbf{p}) & \text{otherwise} \end{cases} \tag{20}$$

with ϕ the "elastic potential" defined by

$$\phi(\mathbf{p}) = \frac{1}{N}\sum_{\mathbf{k}} \Phi(\mathbf{k}) e^{-i\,\mathbf{k}\cdot\mathbf{p}}. \tag{21}$$

Alternatively it can be written in terms of Fourier transforms:

$$E = W_0 + \frac{1}{2N}\sum_{\mathbf{k}} \Psi(\mathbf{k})\ |\Gamma(\mathbf{k})|^2 \tag{22}$$

where $\Psi(\mathbf{k})$ is defined by

$$\Psi(\mathbf{k}) = \sum_{\mathbf{p}} \psi(\mathbf{p}) e^{i\mathbf{k}\cdot\mathbf{p}} = (R_A - R_B)^2\ \Phi(\mathbf{k}) - 2J(\cos a\,k_1 + \cos a\,k_2) \tag{23}$$

Eqn (23) implies that $\psi(\mathbf{0})$ is equal to the $\mathbf{k}$-space average of $\Psi(\mathbf{k})$ (i.e. its average over a Brillouin zone). We shall use this fact later.

Fig. 2. shows some examples of the function $\Psi(\mathbf{k})$. In these examples the ratios of the stiffness constants have been given the values shown in Table 1. The relative magnitude of the elastic and the chemical interactions, as measured by the "elastic misfit parameter"

$$\lambda = (R_A - R_B)^2 \; B/J \tag{24}$$

where B is the bulk modulus defined in eqn (4), has been given the following values: 0 in Fig 2(a), 2.18 in Fig 2(b), 10.9 in Fig 2(c), ∞ in Fig 2(d). The quantity plotted is actually $\Psi(\mathbf{k})/J$ in Figs 2(a,b,c), $\Phi(\mathbf{k})/B$ in Fig 2(d). For $\lambda = 0$ (fig. 2a), the potential close to $\mathbf{k} = 0$ is isotropic, but has a strong quadratic dependence on the length of $\mathbf{k}$. The purely elastic potential (Fig. 2d) on the other hand, depends strongly on the direction of $\mathbf{k}$, but not so much on its length. Fig.2b and 2c are intermediate and show a dependence both on the length and on the direction of $\mathbf{k}$. The same conclusions arise from Fig.3, where sections through the potentials in Fig.2 along (10) and (11) directions are shown.

3 Mean-Field Approximation

3.1 The method

In order to understand better what phenomena might be expected in our model, we develop in this section some predictions given by a non-uniform mean-field approximation (i.e. a phase-field model). In this approximation the state of the system is described by a function over lattice sites $\bar{\gamma}$ such that for each lattice site $\mathbf{p}$ the mean value of the "spin" variable $\gamma(\mathbf{p})$ is $\bar{\gamma}(\mathbf{p})$. It is assumed that the energy E and the entropy S can be written in terms of the quantities $\bar{\gamma}(\mathbf{p})$ in the usual way (see, for example, eqn (18) of [33]), i.e. that the entropy is given by

$$S = -k_B \sum_{\mathbf{p}} f(\bar{\gamma}(\mathbf{p})) \tag{25}$$

where k_B is Boltzmann's constant and f a function of a real variable x

$$f(x) = \left[\frac{1+x}{2} \ln\left(\frac{1+x}{2}\right) + \frac{1-x}{2} \ln\left(\frac{1-x}{2}\right)\right], \tag{26}$$

and that the spins at different sites are statistically independent so that the thermodynamic energy is given, in accordance with (19), by

$$E = W_0 + \frac{1}{2} \sum_{\mathbf{p},\mathbf{p}'} \psi(\mathbf{p} - \mathbf{p}')\bar{\gamma}(\mathbf{p})\bar{\gamma}(\mathbf{p}') + \frac{1}{2}\psi(0) \sum_{\mathbf{p}} [1 - \bar{\gamma}(\mathbf{p})^2]. \tag{27}$$

The second sum corrects for the fact that when $\mathbf{p} = \mathbf{p}'$ the average of $\bar{\gamma}(\mathbf{p})\bar{\gamma}(\mathbf{p}')$ is 1, not $\bar{\gamma}(\mathbf{p})^2$.

3.2 Stability and the critical temperature

We first study the stability of the uniform state, by expanding the Helmholtz free energy $F = E - TS$ in powers of the deviations of the variables $\bar{\gamma}(\mathbf{p})$ from their mean value $2c-1$. Noting that the second derivative of $f(2c-1)$ with respect to $2c-1$ is $f''(2c-1) = 1/4c(1-c)$, and neglecting powers higher than the second, we obtain an expression which can be written in terms of Fourier transforms as

$$F = E - TS \approx F_0 + \frac{1}{2} \sum_{\mathbf{k} \neq \mathbf{0}} |\bar{\Gamma}(\mathbf{k})|^2 \left\{ \frac{k_B T}{4c(1-c)} + \Psi(\mathbf{k}) - \psi(0) \right\} \tag{28}$$

where F_0 is defined by

$$F_0 = W_0 + N k_B T\, f(2c-1) + \frac{1}{2} N \Psi(\mathbf{0})(2c-1)^2 + 2N\psi(\mathbf{0})c(1-c) \tag{29}$$

and $\bar{\Gamma}$ denotes the Fourier transform of $\bar{\gamma}$, defined in analogy with (2).

At high enough temperatures, the coefficient of $|\bar{\Gamma}(\mathbf{k})|^2$ is positive for all $\mathbf{k}$ so that the uniform state (i.e. $\bar{\Gamma}(\mathbf{k}) = 0, \mathbf{k} \neq 0$) is stable. But as the temperature is lowered, one of these coefficients can become negative and the stable state will be non-uniform, that is to say the system will split up into different thermodynamic phases. Since the maximum value of $1/4c(1-c)$ is 1, achieved when $c = 1/2$, such an instability can occur if and only if $T < T_c^{MF}$, where

$$k_B T_c^{MF} = \max_{\mathbf{k} \neq 0} [\psi(\mathbf{0}) - \Psi(\mathbf{k})] \tag{30}$$

that is to say, the maximum of the amount by which $\Psi(\mathbf{k})$ falls short of its $\mathbf{k}$-space average $\psi(\mathbf{0})$. Using (20) and (23), eqn (30) can be written in terms of $\Phi(\mathbf{k})$ as

$$k_B T_c^{MF} = \max_{\mathbf{k} \neq 0} \{(R_A - R_B)^2 [\phi(\mathbf{0}) - \Phi(\mathbf{k})] + 2J(\cos ak_1 + \cos ak_2)\} \tag{31}$$

In the special case where there is no elastic effect (e.g. because $R_A = R_B$) the quantity to be maximized in (31) is simply $2J(\cos ak_1 + \cos ak_2)$ so that we obtain (in the limit of an infinitely large lattice) the usual formula $k_B T_c^{MF} = 4J$. In this case the maximum occurs at the $\mathbf{k}$-value closest to $\mathbf{k} = \mathbf{0}$, correponding to the largest possible wavelength. This indicates that at equilibrium the domains of the two phases are very large. This remains true as long as λ (defined by eq.24) in eq.(31) is small enough, in the case of our numerical example (Table 1) smaller than ≈ 83. In this numerical example, the minimum of the potential switches to $\mathbf{k} = (\frac{1}{2}, 0)$ when $\lambda > 83$, which corresponds to a striped ground state with alternating stripes one atomic spacing thick along either lines or columns. In particilar, this is the ground state when $J = 0$ in eq.(31), that is when there is only elastic interaction (see also Fig.3).

Considering only the case where λ is small enough, the maximum in eq.(31) occurs close to $\mathbf{k} = \mathbf{0}$. Substituting the small-k approximation for Φ, eqn (14), into (30), we obtain (in the limit of an infinitely large lattice)

$$k_B T^{MF} = \max_{\theta} \{(R_A - R_B)^2 [\phi(\mathbf{0}) - Y(\theta)] + 4J\} \tag{32}$$

As we have already noted in our discussion of eqn(15), the maximum is attained at $\theta = \pi/4$ in the case of positive anisotropy ($\Delta > 0$) and at $\theta = 0$ for negative anisotropy. In terms of the elastic misfit parameter λ defined in (24) the ratio of T_c^{MF} to its value in the absence of elastic forces can be written (for the case $\Delta < 0$)

$$\frac{k_B T^{MF}}{4J} = 1 + \left\{ \frac{\phi(\mathbf{0}) - Y(0)}{4B} \right\} \lambda \qquad \text{(small } \lambda) \tag{33}$$

In the case $\Delta > 0$ the $Y(0)$ in this equation is replaced by $Y(\pi/4)$.

In general it is not obvious whether the coefficient of λ in (33) is positive or negative, that is, whether strengthening the elastic interaction increases or decreases the critical temperature. In our numerical example (Table 1) the numbers needed for eq.(33) are

$$\phi(0)/B \approx 0.765 \qquad \text{and} \qquad Y(0)/B \approx 0.529$$

and so the formula becomes

$$\frac{k_B T_c^{MF}}{4J} \approx 1 + 0.059\,\lambda \tag{34}$$

Thus for this particular case the elastic interaction increases the critical temperature, by a percentage of about $5.9\,\lambda$.

The critical temperature we have calculated above is the critical temperature for separation into two coherent phases, that is to say two phases with the same lattice spacing a. It should not be confused with the critical temperature for separation into two incoherent phases, with different lattice spacings. This critical temperature, which we may denote by $T_{c,I}^{MF}$ can be calculated as follows. The free energy of a homogeneous phase with concentration c in which the lattice spacing takes the value that minimizes the free energy for that particular value of c is equal to F_0 as given by (29), and the critical temperature for separation into two such phases is the temperature at which this function ceases to be a convex function of c, i.e. the highest temperature at which d^2F_0/dc^2 takes the value 0 for some c. The relevant value of c is 1/2 and the corresponding temperature is, by (29),

$$\begin{aligned} T_{c,I}^{MF} &= \psi(\mathbf{0}) - \Psi(\mathbf{0}) - \frac{1}{4N} W_0''(1/2) \\ &= 4J + (R_A - R_B)^2 \{\phi(\mathbf{0}) - w_0\} \end{aligned} \tag{35}$$

where W_0'' denotes the second derivative of W_0 with respect to c, and w_0 is defined and calculated in Appendix 3 (eq.11). For the numerical example (see Table 1) we obtain

$$\frac{k_B T_{c,I}^{MF}}{4J} \approx 1 + 0.176\,\lambda \tag{36}$$

This may be compared with the expression (34), showing that $T_{c,I}^{MF}$ is greater than T_c^{MF}, i.e. the requirement of coherence lowers the critical temperature. In this sense, then, the elastic interactions reduce the critical temperature, as pointed out by Cahn [34]. This is illustrated in Fig.4, where both expressions (34) and (36) as well as $T_c^{MF}/T_{c,I}^{MF}$ are plotted as functions of λ.

The above considerations can be extended to give a "phase diagram" for the instability. If c is fixed, then eqn (28) shows that the instability appears as soon as the temperature is less than $4c(1-c)T_c^{MF}$ with T_c^{MF} defined as in (30). If this maximum temperature is plotted against c we get a parabolic curve similar to the usual phase diagrams in mean field theory. It is also possible to obtain a phase diagram for the separation into incoherent phases, by applying the normal methods of mean-field theory to the free energy function F_0. The coexistence curve is given by the values of c for which $dF_0/dc = 0$ with $d^2F_0/dc^2 > 0$, and the spinodal curve by the points at which $d^2F_0/dc^2 = 0$.

3.3 Growth of unstable modes

Besides the equilibrium properties, we can also use the free energy formula (28) to discuss the growth of unstable modes in the early stages of spinodal decomposition. We start with the Cahn-Hilliard kinetic equation for a lattice system, which can be written (see, for example, eqn(31) of [33])

$$\frac{\partial\bar{\gamma}(\mathbf{p})}{\partial t} = a^{-2}M \; \triangle \, \frac{\partial F}{\partial\bar{\gamma}(\mathbf{p})} \tag{37}$$

where M is a constant accounting for the atomic mobility and $\triangle$ is the finite difference Laplacian. The Fourier transform of $\triangle$ is

$$e^{i\,ak_1} - 2 + e^{-i\,ak_1} + e^{i\,ak_2} - 2 + e^{-i\,ak_2} = -2\,(2 - \cos ak_1 - \cos ak_2),$$

or $-2\,(v+w)$ in the notation of eq.(13). Linearizing (37) with respect to $\bar{\gamma}(\mathbf{p})$ and taking the Fourier transform, we obtain with the help of (28)

$$\frac{\partial}{\partial t}\bar{\Gamma}(\mathbf{k}) = 2\,a^{-2}\,J\,M\,\zeta(\mathbf{k})\,\bar{\Gamma}(\mathbf{k}) \tag{38}$$

where

$$\begin{aligned} J\,\zeta(\mathbf{k}) &= -(v+w)\left\{\frac{k_B T}{4c(1-c)} + \Psi(\mathbf{k}) - \psi(0)\right\} \\ &= -(v+w)\left\{\frac{k_B T}{4c(1-c)} - 2J(2-v-w) + (R_A - R_B)^2[\Phi(\mathbf{k}) - \phi(\mathbf{0})]\right\}; \end{aligned} \tag{39}$$

in the second line we have used (23) and (20). Below the temperature $4c(1-c)T_c^{MF}$ mentioned in the preceding section, $\zeta(\mathbf{k})$ is positive for some values of $\mathbf{k}$ and the corresponding modes are unstable. According to the linearized theory of spinodal decomposition [34], one may expect $\Gamma(\mathbf{k})$ for these modes to grow with time t as $\exp(2a^{-2}JM\,\zeta(\mathbf{k})\,t)$ in the very first moments after the quench. The most unstable mode is the one that maximizes $\zeta(\mathbf{k})$.

The (dimensionless) amplification factor $\zeta(\mathbf{k})$ is plotted for several choices of λ (defined in eq.24) and $T/T_c^{MF} = 0.45$ in Fig. 5. It is apparent that the symmetry of the k-space potential (see Fig.2) is reflected in these curves. Moreover, the most unstable mode is at a finite k and independent of direction when λ=0, that is when there is no elastic misfit. As soon as $\lambda \neq 0$, the most unstable mode is found in (10) and (01) directions, in agreement with the discussion in sect.2.2.

To compare the formulas (38) and (39) with those obtained by Cahn [5] from a continuum model, we can use the small-**k** approximation implied by (14), which can be written

$$\Phi(\mathbf{k}) = Y(\theta) + Z(\theta)k^2 + \dots \tag{40}$$

where $Z(\theta)$ is a function whose explicit form we do not need. Using this approximation in (39), we obtain to order k^4

$$J\zeta(\mathbf{k}) = -\frac{1}{2}k^2\{\frac{k_B T}{4c(1-c)} - 4J + (R_A - R_B)^2[Y(\theta) - \phi(\mathbf{0})] + [2Ja^2 + (R_A - R_B)^2 + Z(\theta)]k^2\}; \tag{41}$$

The term $2Ja^2$ in the coefficient of k^2 has its counterpart in Cahn's analysis, where it arises from a term in the free energy proportional to the square of the gradient of c, but the anisotropic $Z(\theta)$ term, arising from features of the elastic interaction that do not show up in the elastic continuum approximation, is new.

4 A procedure for Kawasaki dynamics

In our simulations we allowed the configuration of the system to evolve by means of Kawasaki dynamics with the Metropolis rule [32]. To execute one step of this evolution, choose a nearest-neighbour pair of atoms at random and calculate the energy change δE that their exchange would entail. If this energy is negative, carry out the exchange ; if it is positive, carry out the exchange with probability $\exp(-\delta E/k_B T)$.

We used the following procedure to calculate δE. First choose a large integer C (typically 10^4) and define

$$\tilde{\psi}(\mathbf{p}) = \text{ integer nearest to } C\psi(\mathbf{p}) \tag{42}$$

Then define

$$\begin{aligned} D_i^1(\mathbf{p}) &= \tilde{\psi}(\mathbf{p} + a\mathbf{e}_i) - \tilde{\psi}(\mathbf{p}) \quad (i \in \{1,2\}) \\ D_{ij}^2(\mathbf{p}) &= D_i^1(\mathbf{p}) - D_i^1(\mathbf{p} - a\mathbf{e}_j) \quad (i,j \in \{1,2\}) \end{aligned} \tag{43}$$

Let the chosen nearest-neighbour pair be $\mathbf{p}_0$ and $\mathbf{p}_0 + \mathbf{e}_i$. We may assume that the atoms at these positions are different (otherwise no exchange can be made), so that $\gamma(\mathbf{p}_0 + \mathbf{e}_i) = -\gamma(\mathbf{p}_0)$. The energy change that an exchange would entail can be calculated from (17). To accuracy $1/C$, it can be written

$$\delta E = C^{-1}[\,\gamma(\mathbf{p}_0)\; H_i(\mathbf{p}_0) + 4\; D_i^1(0)] \tag{44}$$

where

$$H_i(\mathbf{p}) = 2\sum_{\mathbf{p}'} \gamma(\mathbf{p}')\, D_i^1(\mathbf{p} - \mathbf{p}').$$

The second term in (44) corrects for the fact that the interaction between the two atoms that have been exchanged does not change sign.

The arrays $D_i^1(\mathbf{p})$, $D_{ij}^2(\mathbf{p})$ and $H_i(\mathbf{p})$ having been stored in the computer, the energy change is easily found by looking up $H_i(\mathbf{p}_0)$.

Each time an exchange is actually carried out, the matrices H_1 and H_2 must be updated. Let us assume that an exchange of atoms at $\mathbf{p}_0$ and $\mathbf{p}_0 + e_i$ has taken place; then H_1 and H_2 change by

$$\delta H_j(\mathbf{p}) \quad = \quad 4 \ \gamma(\mathbf{p}_0) \ D^2_{ji}(\mathbf{p} - \mathbf{p}_0) \quad (j \in \{1, 2\}) \tag{45}$$

An important feature is that the elements of the matrices H_1 and H_2 are integers. Consequently, the updating can be done using integer arithmetic, which is fast and also avoids the accumulation of rounding errors which would otherwise become very serious in a long Monte Carlo run.

Since the arrays $D^1_i(\mathbf{p})$ and $D^2_{ij}(\mathbf{p})$ do not change during the time evolution, they can be computed at the beginning of the run and stored permanently. Moreover, since $D^2_{ij}(\mathbf{p})$ is an approximation to a rapidly decreasing function of $|\mathbf{p}|$, it is zero for large $|\mathbf{p}|$. Thus the matrix needed for the updating is smaller than the full lattice, with a corresponding saving of computing time. The computer code implementing these procedures on a 64x64 square lattice turned out to be only about five to ten times slower than the corresponding standard program for the Ising model with short-range interactions.

The results of these simulations will be described in Part II.

Appendix 1

The total elastic energy W can be expressed as the sum of contributions from N 'plaquettes', a typical plaquette being the square with vertices $(A, B, C, D) = (\mathbf{p}, \mathbf{p} + a\mathbf{e}_1, \mathbf{p} + a(\mathbf{e}_1 + \mathbf{e}_2), \mathbf{p} + a\mathbf{e}_2)$ (see Fig.5). The energies of the springs along the edges of a plaquette are shared equally between the two plaquettes that meet there. We define three vectors $\mathbf{f} = (f_1, f_2), \mathbf{g} = (g_2, g_2), \mathbf{h} = (h_1, h_2)$, by

$$\begin{aligned}
\mathbf{f} &= \frac{1}{2}[-\mathbf{u}_A + \mathbf{u}_B + \mathbf{u}_C - \mathbf{u}_D] \\
\mathbf{g} &= \frac{1}{2}[-\mathbf{u}_A - \mathbf{u}_B + \mathbf{u}_C + \mathbf{u}_D] \\
\mathbf{h} &= \frac{1}{2}[\mathbf{u}_A - \mathbf{u}_B + \mathbf{u}_C - \mathbf{u}_D]
\end{aligned} \tag{A1}$$

For simplicity, we consider the case where the atoms are all of the same size, so that $\eta(\mathbf{p}) = 0$ for all $\mathbf{p}$. The contribution to W, as defined in formula (6), from the plaquette ABCD can then be written

$$\begin{aligned}
\delta W &= \frac{1}{4}L_+[(f_1 - h_1)^2 + (f_1 + h_1)^2 + (g_2 - h_2)^2 + (g_2 + h_2)^2] + \\
&\quad + \frac{1}{4}T_+[(f_2 - h_2)^2 + (f_2 + h_2)^2 + (g_1 - h_2)^2 + (g_1 + h_1)^2] + \\
&\quad + \frac{1}{4}L_\times[(f_1 + f_2 + g_1 + g_2)^2 + (f_1 - f_2 - g_1 + g_2)^2] \\
&= \frac{1}{2}(L_+ + L_\times)(f_1^2 + g_2^2) + \frac{1}{2}(T_+ + L_\times)(f_2^2 + g_1^2) + \\
&\quad + \frac{1}{2}(L_+ + T_+)(h_1^2 + h_2^2) + L_\times f_1 g_2 + L_\times f_2 g_1
\end{aligned} \tag{A2}$$

This expression can be rearranged to give

$$\begin{aligned}
\delta W &= \frac{1}{2}(L_+ + L_\times)(f_1^2 + g_2^2) + (L_\times - T_+)f_1 g_2 + \frac{1}{2}(T_+ + L_\times)(f_2 + g_1)^2 \\
&\quad + \frac{1}{2}(L_+ + T_+)(h_1^2 + h_2^2) + T_+(f_1 g_2 - f_2 g_1) \qquad \text{(A3)}
\end{aligned}$$

The last term can rewritten, using the identity

$$\begin{aligned}
f_1 g_2 - f_2 g_1 &= (\mathbf{f} \times \mathbf{g}) \cdot \mathbf{k} \\
&= \frac{1}{2}(\mathbf{u}_A \times \mathbf{u}_B + \mathbf{u}_B \times \mathbf{u}_C + \mathbf{u}_C \times \mathbf{u}_D + \mathbf{u}_D \times \mathbf{u}_A) \cdot \mathbf{k} \qquad \text{(A4)}
\end{aligned}$$

where $\mathbf{k}$ is a unit vector perpendicular to the plane of the lattice. When the expressions (A4) for all the plaquettes on the lattice are added up, the total is zero since each term such as $\mathbf{u}_A \times \mathbf{u}_B$ is cancelled by an equal and opposite term from a neighbouring plaquette

To interpret the remaining terms in (A3) in terms of continuum elasticity, we regard $\mathbf{p}$ as a continuous variable and use Taylor's expansion to represent $\mathbf{u}_A$, etc. in terms of $\mathbf{u}$ and its derivatives at the mid-point of the plaquette. This gives, using (A1), the approximations

$$\begin{aligned}
\mathbf{f} &\approx a\partial\mathbf{u}/\partial x_1 + O(a^3) \\
\mathbf{g} &\approx a\partial\mathbf{u}/\partial x_2 + O(a^3) \\
\mathbf{h} &\approx a^2\partial^2\mathbf{u}/\partial x_1 \partial x_2 + O(a^4)
\end{aligned} \qquad \text{(A5)}$$

Using these approximations in (A3), summing over the whole lattice with the help of (A4) and approximating the sum by an integral, we obtain

$$\begin{aligned}
W \approx \int dp_1 dp_2 [\quad & \frac{1}{2}(L_+ + L_\times)(u_{1,1}^2 + u_{2,2}^2) \\
+ \quad & (L_\times - T_+)\, u_{1,1} u_{2,2} \\
+ \quad & \frac{1}{2}(T_+ + L_\times)(u_{1,2} + u_{2,1})^2 \quad]\,(1 + O(a^2))
\end{aligned} \qquad \text{(A6)}$$

where $u_{i,j}$ means $\partial u_i/\partial x_j \quad (i, j \in \{1, 2\})$. Formula (A7) is, to leading order, the elastic energy of a plane elastic medium in which the local displacement is $\mathbf{u}(\mathbf{p})$ and the elastic constants c_{11}, c_{12}, c_{44} are given by (3).

Appendix 2

The length of a spring connecting the atoms near sites $\mathbf{p}$ and $\mathbf{p}'$ is $|\Delta\mathbf{u} + \Delta\mathbf{p}| - [R(\mathbf{p}') + R(\mathbf{p})]$, where $\Delta\mathbf{p}$ means $\mathbf{p}' - \mathbf{p}$, and $\Delta\mathbf{u}$ means $\mathbf{u}(\mathbf{p}') - \mathbf{u}(\mathbf{p})$. The longitudinal energy of this spring is therefore (with $\kappa = +$ or $\times$)

$$\frac{1}{2}L_\kappa[|\Delta\mathbf{u} + \Delta\mathbf{p}| - [R(\mathbf{p}') + R(\mathbf{p})] - l_\kappa]^2$$

$$= \frac{1}{2} L_\kappa \left[\left(\eta_\kappa(\mathbf{p}) + \eta_\kappa(\mathbf{p}') - \Delta u_\parallel \right)^2 - \left(\eta_\kappa(\mathbf{p}) + \eta_\kappa(\mathbf{p}') \right) \Delta u_\perp^2 / |\Delta \mathbf{p}| + O(|\mathbf{u}|^3) \right] \qquad \text{(A7)}$$

where L_κ is the longitudinal stiffness and l_κ the unstretched length of the spring, $\Delta u_\parallel$ and $\Delta u_\perp$ are the components of $\Delta \mathbf{u}$ parallel and perpendicular to $\Delta \mathbf{p}$, and $\eta_\kappa(\mathbf{p})$ is defined to be

$$\eta_\kappa(\mathbf{p}) = R(\mathbf{p}) + \frac{1}{2} l_\kappa - \frac{1}{2} |\Delta \mathbf{p}| \qquad \text{(with } \kappa = + \text{ or } \times) \qquad \text{(A8)}$$

It will turn out that η_κ has the same order of magnitude as $|\mathbf{u}|$, so that the term involving $\Delta u_\perp$ has order of magnitude $O(|\mathbf{u}|^3)$ and can be neglected.

The transverse energy of the spring is not affected by the sizes of the atoms, being given simply by $\frac{1}{2} T_\kappa \Delta u_\perp^2$ where T_κ is the transverse stiffness.

Appendix 3

The c-dependence of the lattice constant a can be found by minimizing the elastic energy (6) with respect to a. This gives

$$a = \frac{L_+ l_+ + \sqrt{2}\, L_\times l_\times + 2(L_+ + \sqrt{2}\, L_\times)\, \bar{R}}{L_+ + 2 L_\times} \qquad \text{(A9)}$$

where

$$\bar{R} = c R_A + (1 - c) R_B.$$

This yields

$$\begin{aligned} \eta_+^0 &= \frac{L_\times \sqrt{2}}{L_+ + 2L_\times} \left(\frac{l_+}{\sqrt{2}} - \frac{l_\times}{2} + (\sqrt{2} - 1)\, \bar{R} \right) \\ \eta_\times^0 &= \frac{-\, L_+}{L_+ + 2L_\times} \left(\frac{l_+}{\sqrt{2}} - \frac{l_\times}{2} + (\sqrt{2} - 1)\, \bar{R} \right) \end{aligned} \qquad \text{(A10)}$$

Consequently, by (11),

$$W_0''(c) = 4N\, (R_A - R_B)^2\, w_0 \qquad \text{(A11)}$$

where

$$w_0 = 2\, (3 - 2\sqrt{2})\, \frac{L_+\, L_\times}{L_+ + 2L_\times}$$

In our numerical example (Table 1) the value of w_0 is 0.061.

References

[1] J.D. Eshelby, *Prog. Solid Mech.* **2**, 89 (1961).

[2] A.J. Ardell, R.B. Nicholson and J.D. Eshelby, *Acta metall.* **14** 1295 (1966).

[3] A.G. Khachaturyan, *Theory of Structural Transformations in Solids* (Wiley, New York, 1983).

[4] J.W. Cahn, *Acta Metall.* **9**, 795 (1961).

[5] J.W. Cahn, *Acta Metall.* **10**, 179 (1962).

[6] A. Onuki and H. Nishimori, *Phys.Rev.B* **43**, 13649 (1991).

[7] H. Nishimori and A. Onuki, *Phys. Rev. B* **42**, 980 (1990).

[8] Y. Wang, L.Q. Chen and A.G. Khachaturyan, *Acta Metall. Mater.* **41**, 279 (1993).

[9] P.H. Leo, W.W. Mullins, R.F. Sekerka and J. Viñals, *Acta Metall. Mater.* **38**, 1573 (1990).

[10] W.C. Johnson, *Acta metall.* **32**, 465 (1984).

[11] T.A. Abinandanan and W.C. Johnson, *Acta Metall. Mater.* **41**, 17 (1993).

[12] P.W. Voorhees, G.B. McFadden and W.C. Johnson, *Acta Metall. Mater.* **40**, 2979 (1992).

[13] K. Kawasaki and Y. Enomoto, *Physica* **A150**, 463 (1988); Y. Enomoto and K. Kawasaki, *Acta Metall.* **37**, 1399 (1989).

[14] J. Gayda and D.J. Srolovitz, *Acta Metall.* **37**, 641 (1989).

[15] R. Wagner, R. Kampmann, in *Phase Transformations in Materials*, edited by P. Haasen (VCH, Weinheim, 1991), Vol. 5, Chap. 4.

[16] T. Miyazaki, M. Doi and T. Kozaki, *Solid State Phen.* **3** 158 (1988).

[17] T. Miyazaki and M. Doi, *Mater. Sci. Eng.* **A110**, 175 (1989).

[18] A. Maheshwari and A.J. Ardell, *Phys. Rev. Lett.* **70**, 2305 (1993).

[19] H.A. Calderon, M.E. Fine and J.R. Weertman, *Metall. Trans.* **A19**, 1135 (1988).

[20] H.Calderon and G.Kostorz, in *Neuton Scattering for Materials Science*, S.M.Shapiro, S.C.Moss and J.D.Jorgensen eds., Mat.Res.Soc.Symp.Proc.**166**, 219 (1990).

[21] A.D.Sequeira, H.A.Calderon and G.Kostorz, *Scr. Metall. Mater.* **30**, 7 (1994).

[22] M. Fährmann, P. Fratzl, O. Paris, E. Fährmann and W.C. Johnson, *Acta Metall. Mater.*, in press.

[23] P. Fratzl, F. Langmayr, G. Vogl and W. Miekeley, *Acta Metall. Mater.* **39**, 753 (1991).

[24] F. Langmayr, P.Fratzl, G.Vogl and W. Miekeley, *Phys. Rev. B*, **49**, 11759 (1994).

[25] W.Hein, *Acta Metall.* **37**, 2145 (1989).

[26] J.S. Langer, M. Bar-on and H.D. Miller, *Phys. Rev.* **A11**, 1417 (1975).

[27] For reviews see K. Binder, in *Materials Science and Technology*, edited by P. Haasen (VCH, Weinheim, 1991), Vol. 5, Chap. 7;
J.D. Gunton, M. San Miguel and P.S. Sahni, in *Phase Transitions and Critical Phenomena*, edited by C. Domb and J.L. Lebowitz (Academic Press, New York, 1983), Vol. 8.

[28] J. Marro, J.L. Lebowitz and M.H. Kalos, *Phys. Rev. Lett.* **43**, 282 (1979); P. Fratzl, J.L. Lebowitz, O. Penrose, J. Amar, *Phys. Rev. B* **44**, 4794 (1991).

[29] M. Born and K. Huang, *Dynamical Theory of Crystal Lattices*, Oxford Univ. Press, 1954.

[30] A.G. Khachaturyan, *Soviet Phys. Crystallogr.* **10**, 246 (1965).

[31] H.E. Cook and D. DeFontaine, *Acta Metall.* **17**, 915 (1969).

[32] K. Binder and D.W. Heermann, *Monte Carlo Simulation in Statistical Physics*, Spinger, Berlin (1988).

[33] O. Penrose, *J. Stat. Phys.* **63**, 975 (1991).

[34] J.W. Cahn, *Trans. Met. Soc. AIME* **242**, 166 (1968).

Table 1:

Table 1: Numerical values chosen for the stiffness constants defined in figure 1. In this table B is the bulk modulus and Δ is the elastic anisotropy parameter given by eqs.(4) and (16), respectively. The numerical values are chosen such that the elastic constants of the two-dimensional model are proportional to those known for (three-dimensional) copper.

	spring model	equivalent elastic model	numerical value
	$(L_\times + L_+)/B$	c_{11}/B	1.16
	$(L_\times + T_+)/B$	c_{44}/B	0.52
	$(L_\times - T_+)/B$	c_{12}/B	0.84
	L_+/B	$(2\,c_{11} - c_{12} - c_{44})/(2\,B)$	0.48
	$L_\times/B$	$(c_{44} + c_{12})/(2\,B)$	0.68
	T_+/B	$(c_{44} - c_{12})/(2\,B)$	-0.16
$\Delta =$	$(L_+ - T_\times - 2L_\times)/(L_\times + T_+)$	$(c_{11} - c_{12} - 2\,c_{44})/c_{44}$	-1.38

Figure Captions

Figure 1: Elastic bonds between a given atom (full circle) and its nearest (thick lines) and next nearest (thin lines) neighbors. L_+ and $L_\times$ are the stiffness constants for stretching or compressing the bonds and T_+ is the stiffness for bending the nearest-neighbour bond.

Figure 2: Total potential $\Psi(\mathbf{k})/J$ (eq.13) for (a) $\lambda = 0$, (b) $\lambda = 2.18$, (c) $\lambda = 10.9$ and (d) purely elastic part $\Phi(\mathbf{k})/B$ of the potential with the numerical values of the coupling constants as given in Table 1. The functions are represented by a color code between their minimum and maximum value inside the first Brillouin zone, $\mathbf{k} = 0$ being in the center of each picture.

Figure 3: The same functions as in Fig.2 plotted along the $[\xi\xi]$ and the $[\xi 0]$-directions, with $\xi = a|\mathbf{k}|/2\pi$. In (a)-(c) a minimum is clearly visible close to $\xi = 0$. In (b) and (c) the potential is lower for the $[\xi 0]$-direction. Note that for the purely elastic part of the potential shown in (d) the minimum is at $[\frac{1}{2}0]$. The dotted line is the average of the potential over the Brilloiin zone, that is $\psi(0)/J$ in (a)-(c) and $\phi(0)/B$ in (d).

Figure 4: Coherent (labelled C) and incoherent (labelled I) critical temperatures in the mean field approximation, respectively $k_B T_c^{MF}/4J$ given by eq.(34) and $k_B T_{c,I}^{MF}/4J$ given by eq.(36) plotted as a function of λ. The curve labelled R is the ratio of coherent to incoherent critical temperature $T_c^{MF}/T_{c,I}^{MF}$.

Figure 5: Fluctuation amplification factor $\zeta(\mathbf{k})$ as given by eq.(39) plotted over the first Brillouin zone, for the temperature $T/T_c^{MF} = 0.45$ and (a) $\lambda = 0$, (b) $\lambda = 2.18$ and (c) $\lambda = 10.9$. The center of each picture corresponds to $\mathbf{k} = 0$. Negative values of $\zeta(\mathbf{k})$, corresponding to stable modes, are shown dark blue and unstable modes are color coded as indicated between 0 and the maximum value of $\zeta(\mathbf{k})$.

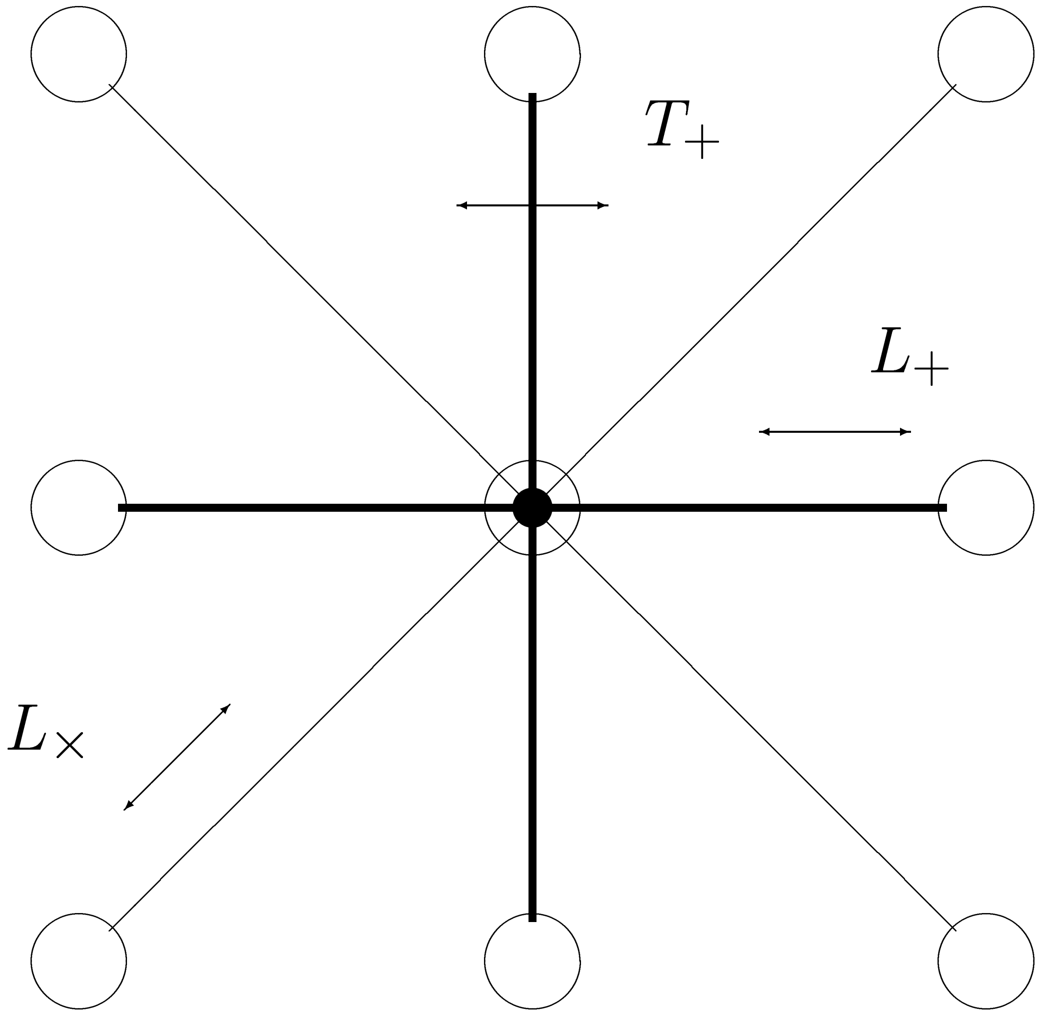

Figure 1.